



A comparison of methods for chemical assessment of reactive silica in concrete aggregates by selective dissolution



X.X. Gao, M. Cyr^{*}, S. Multon, A. Sellier

Université de Toulouse, UPS, INSA, LMDC (Laboratoire Matériaux et Durabilité des Constructions), 135, Avenue de Rangueil, F-31 077 Toulouse Cedex 04, France

ARTICLE INFO

Article history:

Received 14 May 2011

Received in revised form 3 December 2012

Accepted 5 December 2012

Available online 14 December 2012

Keywords:

Alkali-silica reaction

Reactive silica

NaOH attack

HCl attack

HF attack

Selective dissolution

ABSTRACT

This work is a part of a project developing a method to predict the potential expansion of concrete containing alkali-reactive aggregates. The method is based on an original approach which combines laboratory tests on sample cores and finite element calculations to assess the chemical ASR-advancement of aggregates. The chemical advancement of the reaction is linked to the reactive silica content in the aggregates and this work uses chemical methods to evaluate the proportion of reactive silica in different types of aggregates: opal, siliceous limestone, quartzite and quartz aggregate. The evaluation includes (1) mineralogical studies (XRD and petrography) to characterise the reactive sites, (2) chemical methods using acid and/or basic attacks (NaOH–HCl, HCl–KOH, HF) to measure the reactive site content. When these methods are discussed and compared, HF attack is found to give relevant results in short periods of time.

© 2012 Elsevier Ltd. All rights reserved.

1. Introduction

Alkali-silica reaction (ASR) is a chemical reaction occurring in all types of concrete structures, dams, bridges, roads and breakwaters containing alkali reactive aggregates. It is generally admitted that ASR results in two processes [1]: gel formation by alkali solution attacking siloxane bridges, and water absorption by silicate gel causing expansion and damage of the structures. One of the main concerns for structure owners is to know whether the reaction is almost finished or if many years of swelling still remain. An evaluation of the ASR chemical advancement could help the owner to make a reliable choice between different scenarios, including the demolition of the structure or the implementation of repair solutions.

The method of requalification of ASR-damaged structures proposed by Grimal [2] and Sellier et al. [3] is based on a numerical finite element inverse analysis of the structure. One of the basic assumptions of the method is that the potential expansion of the concrete is proportional to the remaining reactive silica within the aggregates. This assumption is based on the consideration that the alkali content is not the limiting parameter of the reaction, since alkalis can be regenerated by calcium ions [4,5] and thus continues to attack the silica [3].

The method of requalification highlights the interest of measuring the quantity of reactive silica in aggregates. However, this

apparently simple question involves complex notions related to the interpretation and the measurement of the so-called “reactive silica”.

1.1. Definition of “reactive silica”

The subjective term “reactive silica” has no absolute meaning since it depends on the conditions of attack (temperature, pressure, type and concentration of solution in contact with silica). Some types of silica known as reactive in a given environment (e.g. in concrete) can be considered as inert or not reactive for other conditions. Obviously, in our context, the term must be taken as the silica that dissolves in contact with concrete pore solution, producing gels leading to the expansion of the concrete. The most common potentially alkali-reactive minerals [6] comprise amorphous and poorly crystalline species like glass, opal, chalcedony, in addition to quartz. Crystal-structural and -chemical details that render certain quartzes alkali-reactive and others innocuous are presently unknown. K-feldspar, mica and other minerals containing alkalis may contribute to deleterious ASR by alkali-release, especially if altered.

1.2. Assessment of reactive silica

The most representative test to evaluate the reactive silica content available for ASR in concrete would simulate real concrete conditions in terms of pH, pressure and humidity temperature. However, under these conditions, ASR usually lasts several decades, even hundreds of years in the case of concrete containing

^{*} Corresponding author. Tel.: +33 561 55 99 06; fax: +33 561 55 99 49.

E-mail address: cyr@insa-toulouse.fr (M. Cyr).

very big aggregates, so the measurement of total silica consumption seems impractical.

A number of accelerated methods are available for rapid chemical assessment of soluble silica in concrete aggregate. Standard chemical methods are used to evaluate the potential reactivity of aggregates, by comparing the dissolved silica with criteria chosen to correspond to ASR-damaged concretes. For instance, ASTM C289 [7] allows the measurement of dissolved silica after crushed aggregates (150–300 μm) are attacked in 1 N sodium hydroxide solution for 24 h at 80 °C. The result obtained is used to classify the aggregate as deleterious or not, but the conditions of test are not intended to measure all the reactive silica.

Other tests are available in the literature to quantify reactive silica but they are initially intended for supplementary cementing materials (SCMs) such as fly ash [8–11], or rice husk ash (RHA) [12]. All these methods, which involve the attack of silica, can be divided into two groups: basic attack and acid attack.

One example of basic attack (other than ASTM C289) is given by Mehta [12], who created the “Silica reactivity index” for RHA, defined as the percentage of available silica which dissolves in an excess of boiling 0.5 N NaOH in 3 min (sample < 45 μm). According to its author, this method gives “an indication of the reactivity of silica present in a material”. However, there is no guarantee that the value obtained concerns the total reactive silica content.

Acid attacks are more commonly found in the literature and different types of acid are used, typically: HCl, HF and organic acids. Sivapullaiah et al. [11] compared the effectiveness of different HCl concentrations (1–5 mol/l) to dissolve silica in fly ash. They found that the results obtained from the concentrations between 2 and 3 mol/l correlated well with the compressive strength of lime/cement fly ashes. Fly ash European standard NF EN 450-1 [13] defines reactive silicon dioxide as the fraction of SiO_2 which is soluble after treatment of the ash with HCl and boiling KOH solution for washing. However, this method, also used for other SCM such as metakaolin [14], sewage sludge ash [15], slag and other pozzolans [16], is sometimes criticised for the uncertainty concerning whether crystalline silica is dissolved [17].

The HF method is usually less criticised, since it allows the amorphous silica to be distinguished from the crystalline form. At the beginning of the HF attack application, researchers focused on finding an appropriate HF concentration and reaction time to attack only the amorphous phase, leaving the crystalline phase [9,18]. However, the results obtained were uncertain, depending mostly on the materials tested in the experiments. For example, Hulett and Weinberger [9] tested fly ashes and concluded that, with 1% HF attack for 16–20 h, the glass phases could be mostly deleted. Diamond [18] tested different types of fly ashes and found that 1% HF and 4 h were the optimised reaction conditions to etch the glass phases. This uncertainty led to unreliability of the results, and a new method was therefore proposed, based on the different dissolution rates of amorphous and crystalline silica. For example, the rate at which quartz dissolved at 25 °C with 0.10 mol/l HF was roughly 2.8–3.0 ($\text{mg m}^{-2} \text{h}^{-1}$), while, for vitreous material under the same attack conditions, the rate was 136–150 ($\text{mg m}^{-2} \text{h}^{-1}$) [19]. This method was successfully used by Murat and Arnaud [20] to measure the amorphous phase of activated kaolinite and montmorillonites, and used by Pichon et al. [21] to quantify the amorphous phase of pozzolanic materials.

Organic methods have been applied to determine the amorphous silica in RHA as a rapid analytical method. One of these methods is based on the mechanism of amorphous silica reacting with glycerol reagent to produce glycerosilicate solution which can be titrated with an aqueous glycerol solution of barium hydroxide. This method has been used only on fine materials up to now. For example, Kreshkov et al. [22] tested it on clay, and Payá et al. [17] used it for testing rice husk ash (size: 10–17 μm).

The aim of this paper is to test and compare three methods, chosen as being simple and rapid, to quantify the amount of reactive silica in four aggregates (including three materials known to be affected by ASR). These methods, which are based on selective dissolution in bases and/or acids, have not been used so far to study alkali-reactive aggregates (or when they have, it was only to evaluate the reactivity to alkalis and not to precisely quantify the proportion of reactive silica). The reliability of the methods is evaluated by correlating the reactive silica contents with expansion measurements of mortars containing the aggregates.

2. Methods and materials

2.1. Methods for the extraction of reactive silica

Three methods, using principles mainly based on a literature review, were used to quantify the amount of potentially reactive silica in aggregates (Fig. 1).

The selective dissolution processes are described in the following sections. They can be divided in two categories: basic attack (NaOH) and acid attack (HCl and HF). Two of the three methods included two steps: a main attack to dissolve the silica contained in the aggregate, followed by a washing phase to dissolve the silica which had precipitated in the first step. During the chemical extraction, the use of glassware was avoided since it could lead to the disturbance of silica dissolution. Steel containers were used for basic attack, porcelain pots for HCl attack and plastic containers for HF attack.

2.1.1. NaOH attack (100 °C and 60 °C) – cold HCl washing

This method is based on US standard ASTM C289 [7] and French standard XP P18-594 [23], since it consists of attacking silica with 1 M sodium hydroxide solution. The use of a basic solution is a reasonable choice to get close to a cement-based environment. These standards were modified for our purposes, since the goal was not to evaluate the reactivity potential of an aggregate but to determine the silica content available for ASR.

Considering the long duration of NaOH attack at ambient temperature, the tests were carried out at a high temperature (100 °C) to accelerate the reaction. The dissolution of silica as a function of reaction time (up to 96 h) was measured on all the materials tested. A few tests were also performed at 60 °C, a temperature usually used in ASR expansion tests [3,15,24].

The aggregate was crushed to particle sizes smaller than 80 μm in order to quickly attack all the silica inside the grains. With coarse particles, the reagent would need a long time to reach the centre of the particles. The analyses of dissolved silica were made with different reaction times for different reaction temperatures (up to 96 h at 100 °C or 150 days at 60 °C) to estimate the kinetics of dissolution. It was assumed that during the reaction time only reactive silica was attacked (this hypothesis is discussed later). The residue of the NaOH attack was then washed with HCl in order to dissolve the gel which was likely to precipitate during the basic attack [25]. If the washing was not performed, some of the dissolved silica which had precipitated could not be measured in solution and this could lead to an underestimation of the reactive silica.

For aggregates containing only small amounts of silica and for which some minerals (e.g. calcite) could interfere with the measurement method (for instance by consuming the reagents), a pre-treatment was conducted to eliminate the matrix and so refine the active fraction. The process, used here with aggregates made of limestone, consisted in dissolving the calcareous part of the aggregate in 0.25 mol/l HCl at 0 °C. The low concentration and low temperature aimed to avoid attacking silica [26]. This kind of

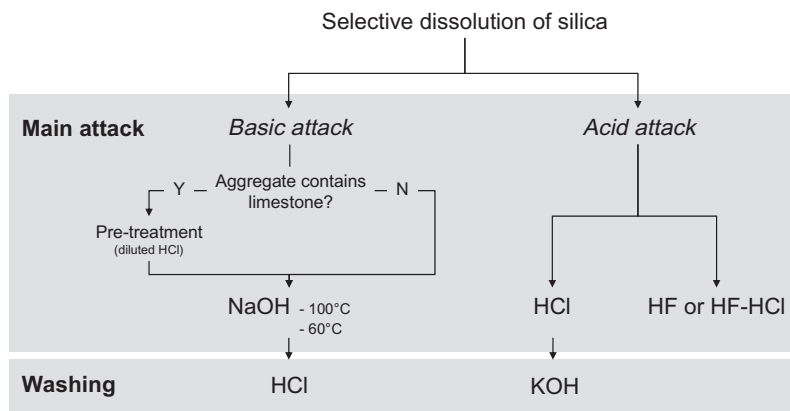


Fig. 1. Methods used to measure the reactive silica content.

pre-treatment is recommended in standards such as French XP P18-594 [23], for limestone contents higher than 15%.

2.1.1.1. Procedure. The procedure of the test is divided in two steps. In the first part, 1.5 g of sample is weighed and put into a 75 ml sealed steel container. After addition 50 ml of 1 mol/l NaOH solution (L/S = 33.3 ml/g), the container is sealed and put in a constant-temperature oven at 100 °C or at 60 °C for different test times. At a given age, the solution is filtered and analysed using atomic absorption. The second step of the test consists in transferring the filtered residue into a beaker, adding 300 ml of cold HCl (1 mol/l), putting the beaker in an ice-water bath (~°C, to avoid silica gel precipitation during the acid attack) for 30 min and then filtrating the solution for SiO₂ measurement by atomic absorption. The total dissolved silica is taken as the sum of the values obtained for the two steps.

2.1.1.2. HCl (heated) – KOH (boiled)

This method is found in standards such as NF EN 450-1 [13] to evaluate the reactive silicon dioxide in fly ash to be used in concrete. Many papers have already reported results using this procedure for other supplementary cementing materials [14–17]. In this method, the aggregate is firstly attacked by concentrated HCl (12 mol/l) in order to destroy the silica network and produce silica gel. KOH (4.5 mol/l) is then used mainly to dissolve the gel and also to attack the remaining reactive silica.

2.1.2.1. Procedure. The procedure of the test is divided into two steps. In the first part, 5 g of sample is weighed and dispersed in a porcelain dish with 125 ml of water. After addition of 200 ml of concentrated HCl (12 mol/l), the solution is evaporated to dryness on a sand bath. The operation is repeated two more times with 100 ml concentrated HCl. Then, the residue is treated with 100 ml diluted HCl (3 mol/l), heated, filtered and washed with boiling water until free from chloride ions. The solution is then analysed using atomic absorption. The second step of the test consists of transferring the residue into a steel container, adding 500 ml KOH (4.5 mol/l) and leaving to stand for 16 h at room temperature. Then the solution is boiled under reflux for 4 h, filtrated, and washed with water and diluted HCl (1.2 mol/l). The solution is analysed for SiO₂ using atomic absorption. The total dissolved silica is taken as the sum of the values obtained for the two steps.

2.1.3. HF attack

This method is found in the literature [9,18,20,21] for the quantification of the amorphous silica in fly ash or pozzolanic materials. It is based on the fact that the amorphous silica dissolves rapidly in

diluted HF solution, and the rate of dissolution can be distinguished from the dissolution of crystalline phases. Different reaction times are obtained, and the kinetics of amorphous phase dissolution can be deduced using a graphic method (Fig. 2).

Considering that some aggregates such as siliceous limestone contain calcite, which can consume HF and interfere with the silica dissolution, a second acid, HCl, was added into HF solution in that case. In this paper, 1 mol/l HCl was chosen to add into 1.5% HF to test siliceous limestone. This second acid is known not to affect the dissolution of silica since Liang and Readey [27] tested the effect of 1 mol/l HCl on fused silica and quartz and found that, with and without HCl, the final values of dissolved silica showed no marked differences.

2.1.3.1. Procedure. 1.5 g of sample were put into a plastic container, mixed with 1.5% HF (or HF + 1 mol/l HCl) in the proportions of 200 ml liquid/g solid, and left for reaction at 4 °C in the aim of obtaining a clear difference between the dissolution of amorphous phase and crystalline phase [27]. At reaction times ranging between 1 and 24 h, the solution was filtered and the residue was washed with distilled water. The solution was then analysed for SiO₂ by atomic absorption.

2.2. Analytical methods and mortar test

2.2.1. Aggregates

The chemical composition of the aggregates was determined using a Perkin Elmer 2100 atomic absorption spectrophotometer with flame atomization. Loss on ignition was measured by

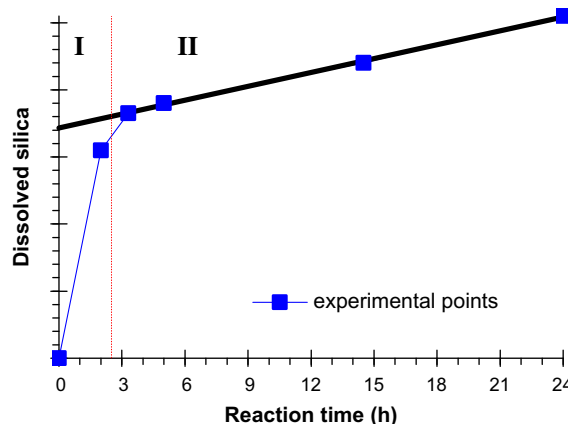


Fig. 2. Typical dissolution kinetics of aggregate in HF.

calcination at 1000 °C. Mineralogical properties were obtained by X-ray powder diffractometry using a Siemens D5000 diffractometer equipped with a monochromator and using a $K\alpha$ ($\lambda = 1.789 \text{ \AA}$) cobalt anticathode. Measurements were made with a 2θ step interval of 0.04° ($5\text{--}70^\circ$) and an acquisition time of 2 s per step. The particle size distribution of the crushed materials used for the dissolution tests was measured by laser granulometry in water, using a Cilas 1090. The petrographic observations by optical microscopy were carried out with thin sections in transmitted light with crossed polars.

2.2.2. Mortars

The potential reactivity of aggregates is usually obtained through the expansion measurement of concrete or mortars conserved at temperature between 40 and 80 °C. Here, expansion was measured on mortar prisms ($20 \times 20 \times 160 \text{ mm}$) with a sand (1612 kg/m^3) to cement (CEM I 52.5R, 538 kg/m^3) ratio of 3. The sand contained 30% of reactive aggregate ($315\text{--}1250 \text{ }\mu\text{m}$) and 70% of non-reactive marble ($0\text{--}2500 \text{ }\mu\text{m}$). The water-cement ratio was 0.5. Mixtures were adjusted to fixed alkali contents ($\text{Na}_2\text{O}_{\text{eq}}$) by adding NaOH in the mixing water in order to have an alkali concentration in the mortar pore solution close to the concentration in the conservation solution (1.0 mol/l). The mortar prisms were demoulded 24 h after casting and were then kept in sealed bags at 20 °C until 14 days of age. At this time, the prisms were immersed in 1 M NaOH solution at room temperature for the 14 following days. After this period, the temperature of the solution was increased to 60 °C. Expansion was measured using the scale micrometre method (specimens had shrinkage bolts at both ends). Each measurement was the mean of three values from three replicate specimens. Expansion measurements were performed after the containers and the prisms had been cooled for 24 h at 20 °C. The ASR-expansions presented in this paper were obtained by subtracting the expansion of a reference mortar (without reactive aggregate, i.e. by using a non-reactive marble) from the total expansion, as already proposed by other authors [28].

2.3. Materials

Four materials were selected for the tests: three aggregates known to be alkali-reactive (siliceous limestone – SL, quartzite – Q, and opal – O), and one material considered as non-reactive (quartz aggregate – QA). The three reactive aggregates were chosen to cover a wide range of types and geological origins, from low to high kinetics of silica dissolution: igneous rock (opal: high kinetics), sedimentary rock (siliceous limestone: low kinetics), metamorphic rock (quartzite: low kinetics). For the chemical tests, the aggregates were crushed to particle sizes of less than $80 \text{ }\mu\text{m}$ (mean diameter of $20 \text{ }\mu\text{m}$). Special attention was paid to avoiding overgrinding of aggregates, in order to limit the appearance of the “soluble surface layer on ground quartz” already observed by other authors (e.g. Iler [19]). This thin amorphous phase around the aggregates could lead to an overestimation of the reactive silica content.

2.3.1. Chemical and mineralogical properties

The chemical compositions of the aggregates are given in Table 1. Quartzite, opal, and quartz aggregate were mainly composed of silica, while the siliceous limestone had only a limited SiO_2 content. In order to identify the forms of reactive silica, petrographic analyses were carried out on each aggregate type.

2.3.1.1. Opal. The XRD pattern of opal (Fig. 3) shows relatively broad diffraction lines at d -spacing between 5.60 and 3.42 \AA . According to the classification proposed by [29], the sample can be considered to be opal-CT, characterised by a structure consisting of randomly interstratified layers of α -tridymite and α -cristobalite [29], with a

Table 1

Chemical compositions of the four aggregates (% by mass).

Aggregates	SiO_2	Al_2O_3	Fe_2O_3	CaO	MgO	Na_2O	K_2O	SO_3	LOI
O	92.7	–	0.3	0.2	0.1	0.2	0.1	1.1	6.0
SL	15.4	1.5	0.7	40.4	1.4	0.4	0.4	4.2	35.6
Q	87.7	4.0	1.0	0.4	0.2	0.1	0.9	0.1	1.1
QA	92.2	3.7	1.1	0.1	0.1	–	0.01	0.2	0.6

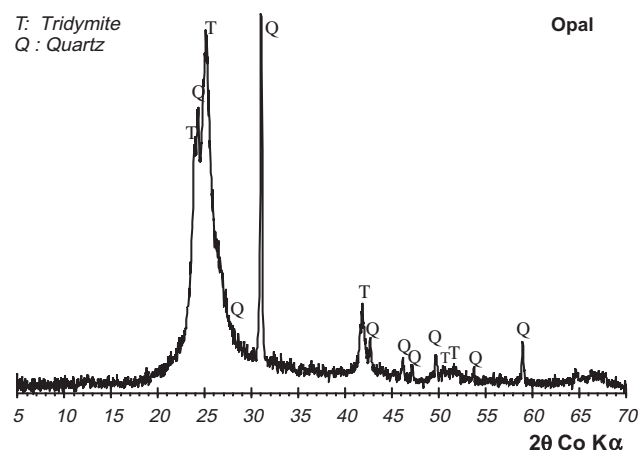


Fig. 3. XRD pattern of opal.

high degree of disorder [30]. Depending on the relative amounts of cristobalite and tridymite, the position of the main opal peak shifts from 4.04 \AA , which is typical of α -cristobalite, to 4.11 \AA , characteristic of α -tridymite. In the sample studied here, the position of the main peak was centred at about 4.11 \AA , closer to the tridymitic one. The well-pronounced secondary peak at 4.3 \AA confirms a high relative amount of tridymite. The XRD pattern also indicates the presence of quartz, confirmed by the diffraction lines at 3.34 and 4.26 \AA .

The petrographic analysis of thin sections (Fig. 4) showed the presence of fibrous chalcedony (A) reaching sizes around $100 \text{ }\mu\text{m}$, surrounded by a glassy phase (B, black in polarised light). Small crystals of xenomorphic quartz (C), presenting a certain degree of undulatory extinction, were also observed.

2.3.1.2. Siliceous limestone. The XRD pattern of SL (Fig. 5) showed that this aggregate was composed of calcite and dolomite, with significant amounts of impurities including quartz, plagioclase feldspars, micas, kaolinite and pyrite. A small amount of amorphous silica was also found in some spectrum patterns, especially visible after HCl pretreatment. In addition to calcite, present in the form of micritic crystals containing many debris of fossils, thin-section observations (Fig. 6) showed the presence of silicified dolomite relic containing microquartz and chalcedony (A), and silicified vein containing chalcedony (B). Amorphous silica was difficult to identify by optical microscopy, but has already been seen in this type of aggregate [31].

2.3.1.3. Quartzite. As shown in the XRD pattern (Fig. 7), quartzite mainly contained quartz, and also a certain amount of phyllosilicate minerals (mica-type such as muscovite). Examination of thin-sections (Fig. 8) showed that this rock was mainly composed of heterometric quartz grains of sizes varying from less than $1 \text{ }\mu\text{m}$ (A) up to a few hundreds of μm (B, C). The presence of primary (C) and recrystallised (B) quartz grains was noted. The former (C) were irregular, showed undulatory extinction and were separated by an intergranular cement (D) composed of microquartz and micas. The latter (B) were usually much better defined and no undulatory

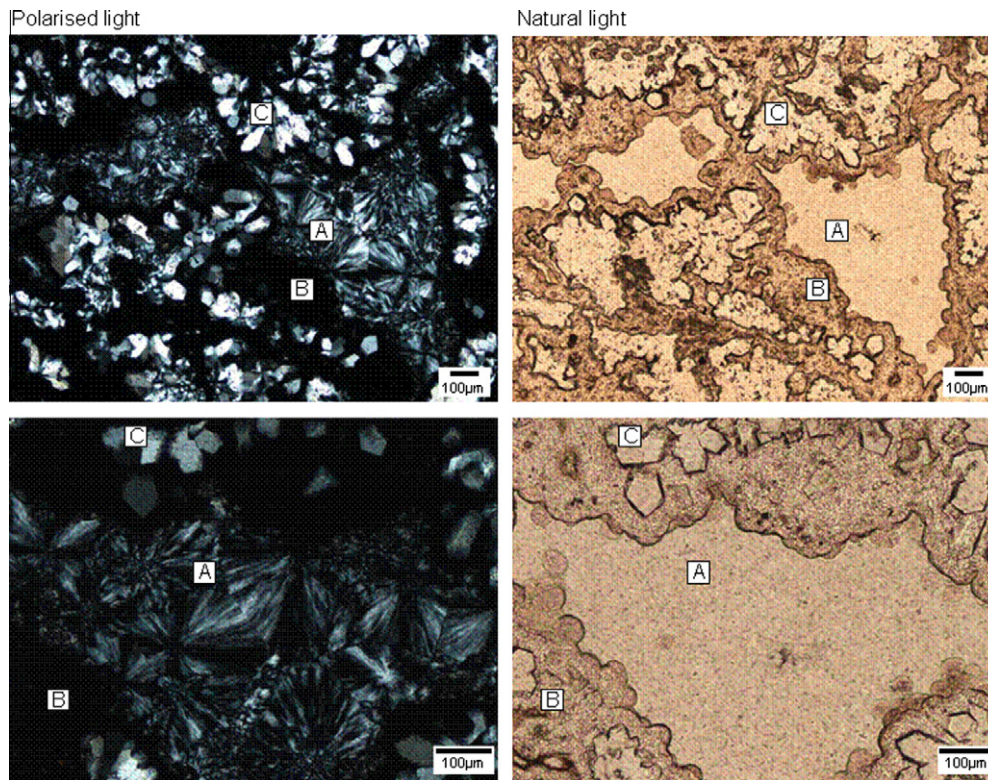


Fig. 4. Thin section micrographs of opal (O) in polarised and natural lights. Fibrous chalcedony (A), builds a spongy framework lined with amorphous opal (B), and locally contains microquartz (C).

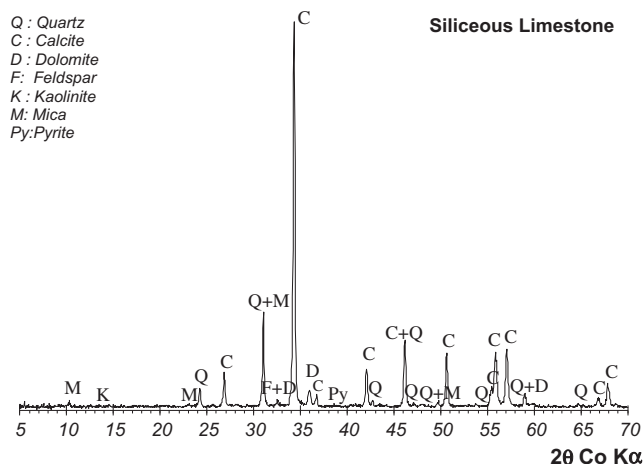


Fig. 5. XRD pattern of siliceous limestone.

extinction was observed. Mica flakes were often found, sometimes concentrated in areas containing microquartz (E), as large particles or as a cementing agent (D). According to Sims and Nixon [32], the intergranular phase is responsible for the alkali-reactivity of this kind of aggregates.

2.3.1.4. Quartz aggregate. The XRD pattern of quartz aggregate (Fig. 9) shows only quartz, with visible traces of other minerals. Thin sections (Fig. 10) reveal:

- (a) Particles composed of quartz grains of a few hundreds of µm, some of them presenting undulatory extinction. Contrary to quartzite, the boundaries of each grain are free of micas or microquartz.

- (b) Large homogeneous quartz grains having a well defined extinction without rolling.

2.3.1.5. Types of silica in aggregates and potential of reactivity. The mineralogical and petrographic studies allowed us to determine the types of silica found in the aggregates. Table 2 summarises the results in terms of qualitative evaluation, with the potential reactivity of each silica type as classified in the literature [32] and [33].

2.3.2. Expansion potential

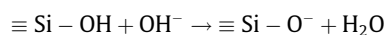
The expansion tests give a good estimation of the difference of reactivity potential of these aggregates (Fig. 11). These results confirm that opal (O), siliceous limestone (SL) and quartzite (Q) are alkali-reactive, and that quartz aggregates (QA) can be considered as a poorly reactive material. The results of the chemical measurements presented below will be compared to these measurements in the final discussion.

3. Results and discussion

3.1. NaOH attack (100 °C and 60 °C) – cold HCl washing

3.1.1. Mechanisms of attack

When silica is exposed to a strong alkaline solution such as NaOH, there is an acid–base reaction between the hydroxyl ions in solution and the acidic silanol (Si–OH) groups [1] as follows:



As further hydroxyl ions penetrate the structure, some of the siloxane linkages (Si–O–Si) are also attacked:



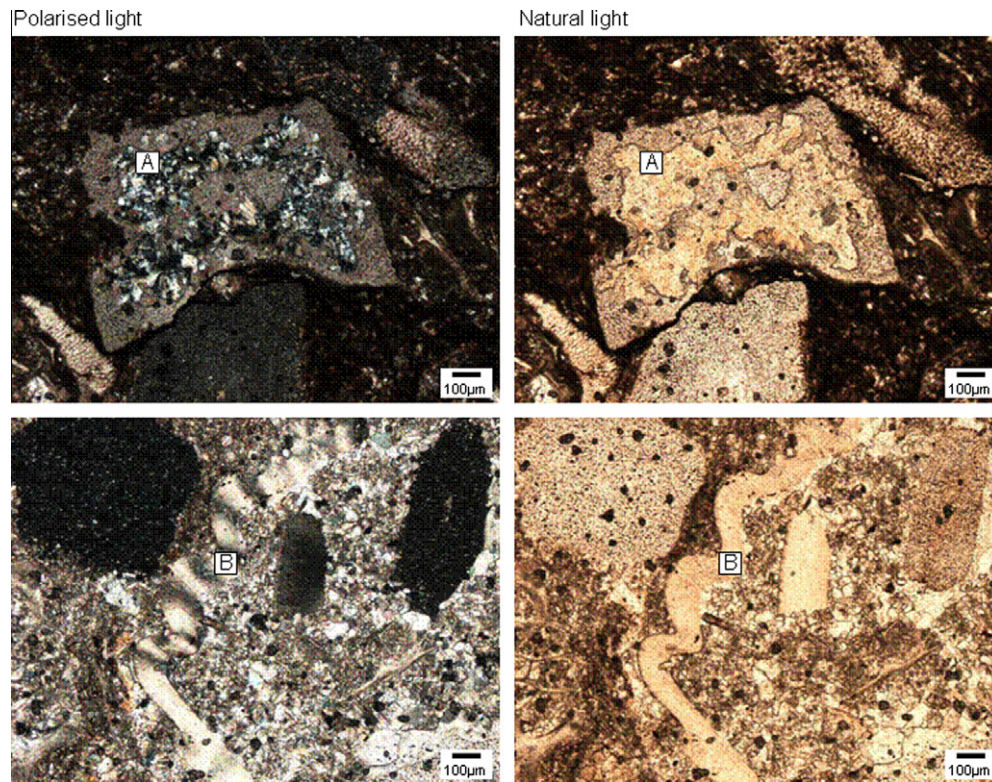


Fig. 6. Thin section micrographs of siliceous limestone (SL) in polarised and natural lights. Silicified dolomite relic containing microquartz and chalcedony (A) and silicified vein containing chalcedony (B).

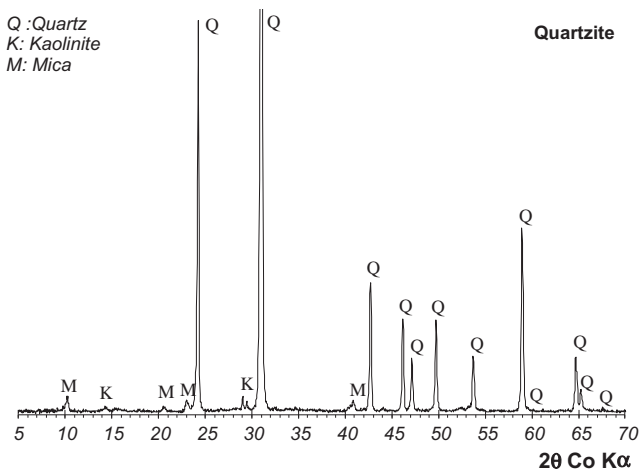


Fig. 7. XRD pattern of quartzite.

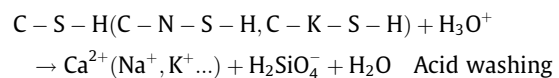
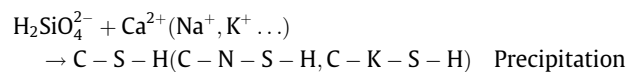
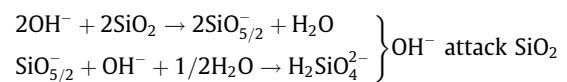
The negative charges on the terminal oxygen atoms are balanced by alkali cations (Na^+) that simultaneously diffuse into the structure. The disruption of siloxane bridges weakens the structure, and if there are sufficient reserves of alkali hydroxide, the process continues to produce an alkaline silicate solution.

This mechanism is suitable for both amorphous silica and crystalline silica but, in this last case, the solubility is much lower. For example, in 25 °C aqueous solution at pH = 14, the solubility of vitreous silica is approximately 21 times the solubility of quartz (~125 mol/l for vitreous silica compared to ~6 mol/l for quartz) [34].

After the dissolution of silica, the calcium ions which exist in the solution (e.g. for siliceous limestone) can favour the precipitation of

the silicate ions to produce a gel [25], thus the HCl washing is conducted to dissolve gel and transfer again the silica into soluble silicate ions.

The reaction mechanism can be simplified as follows [25,35]:



3.1.2. Results

3.1.2.1. Tests at 100 °C. The curves of silica dissolution for the materials after the two steps of the method (NaOH at 100 °C followed by cold HCl washing) are shown in Fig. 12a. The results are presented as the percentage of dissolved silica (by mass) with respect to all the mass of the material. The curves of O, SL and QA reached an asymptote in the measuring times, while the curve of Q was still increasing at the end of the test. To obtain the asymptotic values, all the five curves were fitted by using a typical equation for dissolution:

$$\text{Si}_{\text{dissolved}} = \text{Si}^\infty (1 - e^{-at}) \quad (1)$$

where $\text{Si}_{\text{dissolved}}$ is the amount of silica dissolved at time t , Si^∞ is the asymptotic value for $t = \infty$, and a is a parameter depending on the nature of aggregate.

The Si^∞ value was obtained through curve fitting, and this value was considered to be representative of reactive silica. The kinetics of the silica dissolution can give qualitative information about

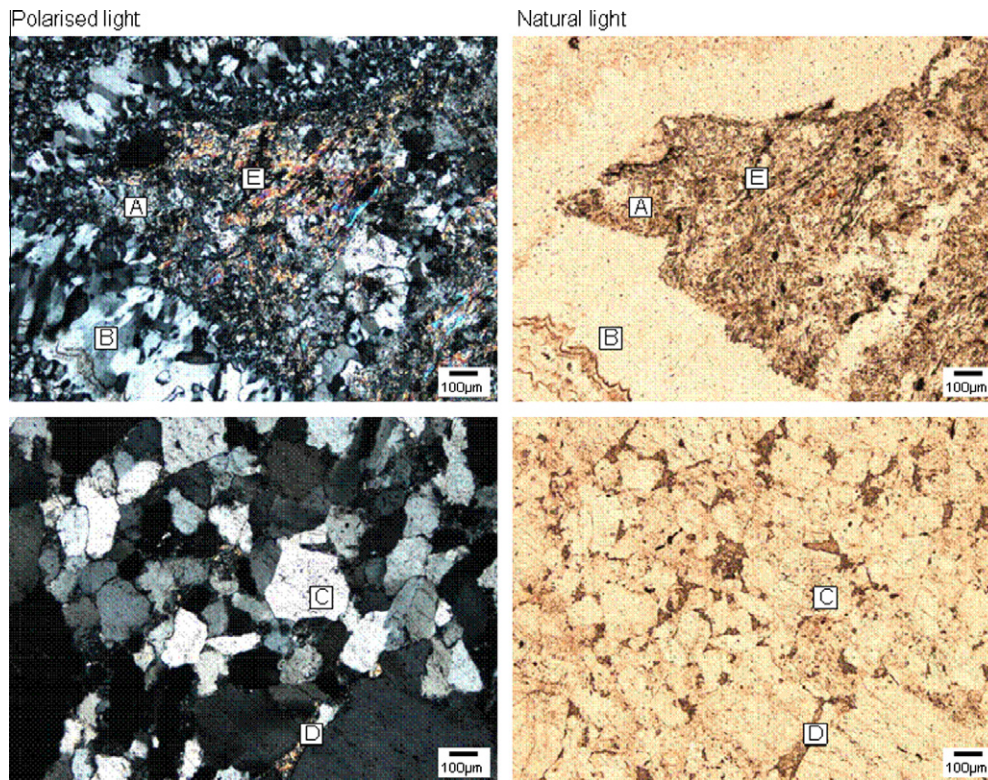


Fig. 8. Thin section micrographs of quartzite (Q) in polarised and natural lights. Low-grade metamorphic quartzite with quartz (A, C) and mica flakes (E) of detrital origin cross-cut by vein quartz (B), and intergranular siliceous cement (D).

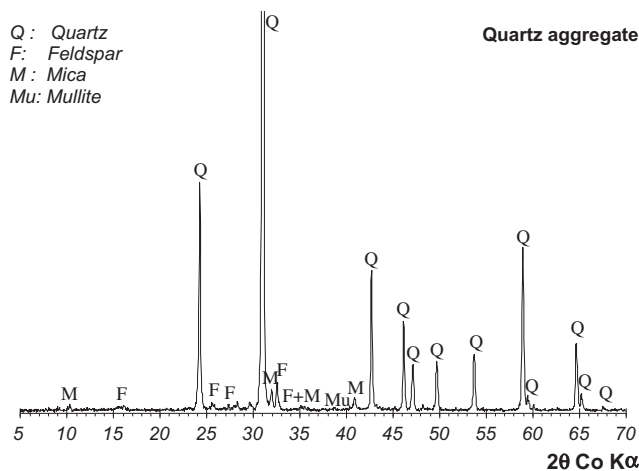


Fig. 9. XRD pattern of quartz aggregate.

reactive components since the different forms of silica show dissimilar kinetics [36]. Thus, the initial reaction rate and the evolution of reaction rate over time were deduced (Fig. 12b) according to the derivative of Eq. (1). The rate of silica dissolution can be interpreted as the consumption rate of reactive sites in the chemical environment, so high rates can be associated with very reactive components.

Among the reactive aggregates, opal gave the highest dissolved silica value (Fig. 12). The initial rate of dissolution was very high, but it decreased rapidly, meaning that the dissolution process was quick. These results are in accordance with the degree of reactivity of this aggregate (Fig. 11) and with the nature of silica determined by petrographic observations (Table 2).

Siliceous limestone (SL) led to 9.5% of dissolved silica, representing almost 2/3 of the silica in this aggregate (9.5%/15.4%).

Quartzite (Q) gave quite a high value of SiO_2 , considering that it was almost exclusively composed of quartz, which was expected to be weakly reactive (Table 2). The value was around 5 times higher than that of SL, which was inconsistent with the expansion results (Fig. 11) showing that Q had a similar reactivity to that of SL. The kinetics of dissolution of Q was slow and the dissolution curves increased continually with the reaction time. This result raised some doubts about whether this method falsely counted part of the crystalline silica as reactive.

Finally, QA gave the lowest value of all, in accordance with the expansion results (Fig. 11).

3.1.2.2. Test at a different temperature (60 °C). Considering the doubts concerning the possible attack of well crystallised silica when NaOH was used at 100 °C (high temperature might increase the solubility of silica), some supplementary tests on aggregate SL were carried out at 60 °C. This temperature corresponded to the one used in accelerated expansion tests.

The results are given in Fig. 13, with reaction times in hours and days when the attacks were carried out at 100 °C and 60 °C respectively. The comparison of these two curves shows that almost the same asymptotic values were found for the two temperatures, meaning that the solubility of the silica was similar at these two different temperatures. Only the kinetics was different since the initial dissolution rate decreased from 1.1 to 0.014%/h when the temperature passed from 100 to 60 °C.

The Arrhenius law (Eq. (2)) was used to calculate the activation energy, using Eq. (3). The rate constants k_1 ($T_1 = 373 \text{ K}$, 100 °C) and k_2 ($T_2 = 333 \text{ K}$, 60 °C) were deduced from the results presented in Fig. 13, by using the initial rate of dissolution ($t = 0$).

$$k = A \exp^{-E_a/RT} \quad (2)$$

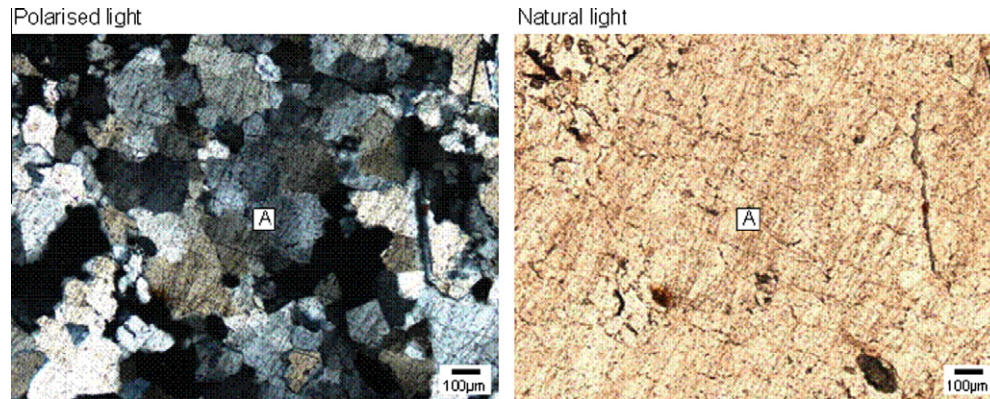


Fig. 10. Thin section micrographs of quartz aggregate (QA) in polarised and natural lights. (A) Quartz.

Table 2

Potential reactivity and occurrence of silica types (related to silica content) in aggregates, obtained by thin section petrography.

Types of silica	Potential of reactivity	Opal	Siliceous limestone	Quartzite	Quartz aggregate
Total content of silica (%)		92.7	15.4	87.7	92.2
Quartz without undulatory extinction	Weak	Scarce	Scarce	Majority	Majority
Quartz with undulatory extinction	Strong	Frequent	Majority	Scarce	Not observed
Microquartz (intergranular)	Strong	Not observed	Scarce	Frequent	Not observed
Chalcedony-like spherulites	Very strong	Frequent	Scarce	Not observed	Not observed
Amorphous phase	Very strong	Frequent	Scarce	Not observed	Not observed

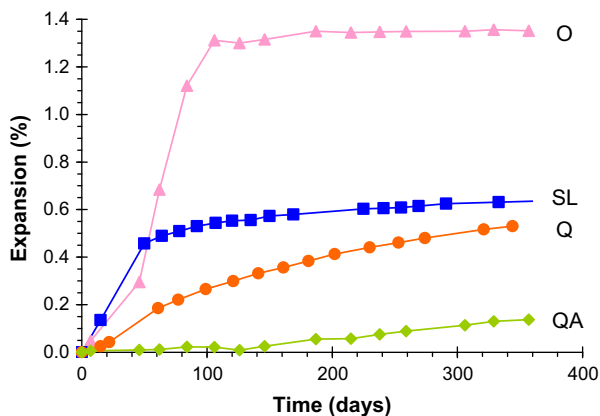


Fig. 11. ASR expansion of mortars containing different types of aggregates.

where k is the rate constant, T the temperature (in Kelvin), E_a the activation energy, A the prefactor and R the gas constant (8.314 J/mol/K).

$$E_a = \frac{R \ln \frac{k_1}{k_2}}{\left(\frac{1}{T_2} - \frac{1}{T_1}\right)} \quad (3)$$

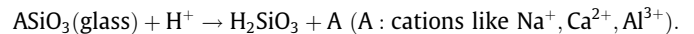
The apparent activation energy E_a calculated was 113 kJ/mol, a value higher than those usually found in the literature (for example 96 kJ/mol [36]). The difference could have been caused by the materials tested and test method. The value here was based on the results of siliceous limestone after NaOH attack and subsequent HCl washing, whereas the value of Dron and Brivot [36] was deduced from the results of opal only after NaOH attack. The precipitation was not taken into account by Dron and Brivot [36]. However, in our work, the precipitation of the silica after the NaOH attack was high as shown in Fig. 14. At 60 °C, only 20% of the silica dissolved by the NaOH attack was in the solution; the rest was in a gel that precipitated in the solution (i.e. 80%, dissolved by the HCl

washing). At 100 °C, 70% of silica was found in the solution, so only 30% was contained in the gel. The large presence of gel at 60 °C could cover the surface of the particle and prevent the dissolution of silica, which could lead to a decrease of k_2 and thus to a higher value of E_a .

3.2. HCl (heated) – KOH (boiled)

3.2.1. Mechanisms of attack

Generally, silicate glasses and silicate minerals can be attacked by acid, leaving a residue of hydrated silica which forms a gel. This process can be explained as the acid removing the iron atoms which are incorporated in the continuous silicon-oxygen frameworks, leaving the siloxane structures to yield gelatinous silica. Paul [34] described the acid attack of silicate glass. Although at lower pH values the exchange of cation with hydrogen ion seems favoured, the silicic acid does not ionise and thus offers a high activation barrier for the diffusion of positive ions. This can explain why only a little soluble silica (<0.1% at 35 °C) is detected in glass in an acid environment.



However, under the conditions of high acid concentration and high temperature, this exchange between cation and hydrogen ion occurs frequently, and finally produces gel. This method was summarised by Iler [19] to synthesise gel by acidifying silicate minerals.

3.2.2. Results

Table 3 presents the results of the HCl attack, followed by the KOH washing. The tests were carried out using particles of less than 80 µm. It should be noted that no soluble silica was measured after the concentrated HCl attack (first stage of the method), since the attacked silica formed a gel that was dissolved only after the KOH washing.

It can be seen from the results that opal (O) again released much more silica (77%) than the other materials. The dissolved silica of

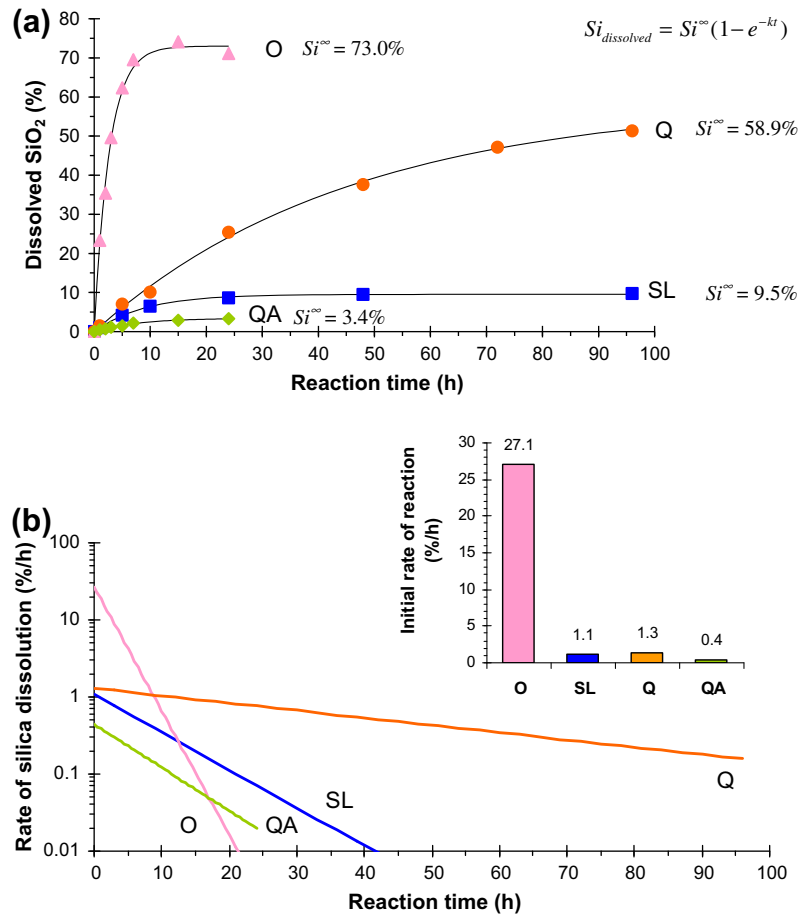


Fig. 12. Dissolved silica (a) and reaction rate (b), as a function of reaction time, after NaOH (100 °C)–HCl attack.

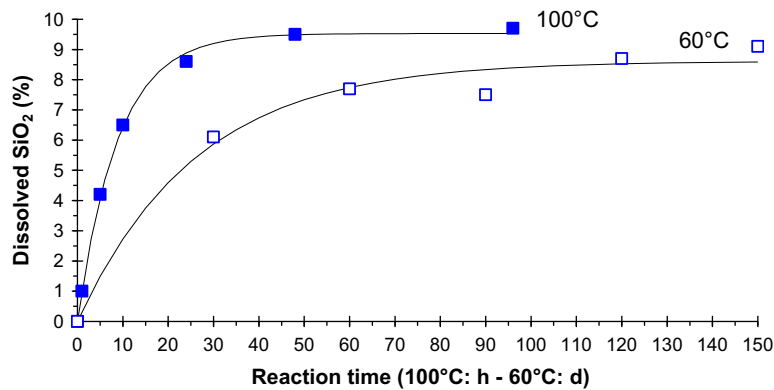


Fig. 13. Dissolved silica of siliceous limestone (SL) as a function of time after NaOH–HCl attack at 60 °C and 100 °C. Note the scale for reaction time: hours at 100 °C and days at 60 °C.

the other reactive aggregates (SL and Q) reached lower values (2.4% and 5.4%, respectively). The non-reactive aggregate QA released 5.4% of its silica, which is the same value as for quartzite. Let us recall that this method, although it is now used for the quantification of active silica and alumina in fly ash (European standard EN 450-1 [13]), was initially intended to measure insoluble residue in cement, as specified in European standard NF EN 196-2 [37]. So it might be accurate for fly ash, but some doubts remain here about its effectiveness in distinguishing between reactive (e.g. quartzite) and non-reactive (e.g. quartz aggregate) aggregates, since it seems

that the extremely severe acid environment favours the attack of well crystallized quartz.

3.3. HF attack

3.3.1. Mechanisms of attack

Fluorine ion is a strong nucleophilic reagent; it has the same mechanism of attack of silicon-oxygen frameworks as OH^- . However, HF is a stronger reagent than alkalis, for two reasons: (1) the electronegativity of F is 3.98, greater than oxygen (3.44), (2)

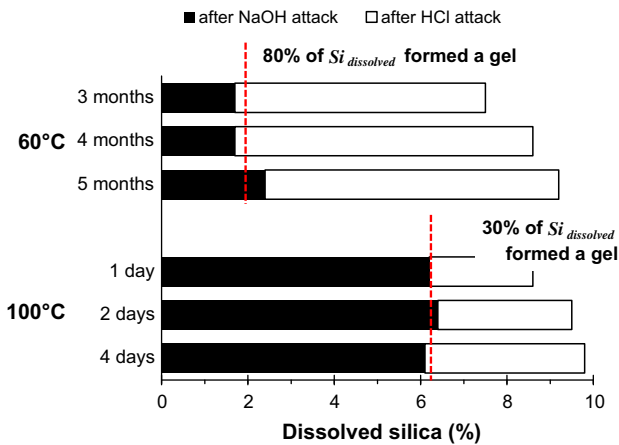


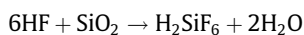
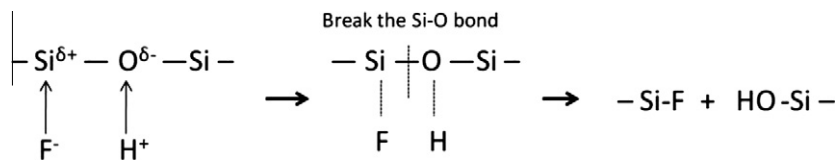
Fig. 14. Comparison of dissolved silica after NaOH and HCl attack at 60 °C and 100 °C.

Table 3
Results of dissolved silica with HCl–KOH method.

	Opal (O)	Siliceous limestone (SL)	Quartzite (Q)	Quartz aggregate (QA)
Dissolved SiO ₂ , in% of the total aggregate mass	77.1	2.4	5.4	5.4

the hydrogen ion (H⁺) as an electrophilic reagent helps fluorine ion to disrupt the Si–O bond [38]. The reaction mechanism is as follows:

The mechanism can be simplified to:



This equation applies at low temperature (<86 °C). At high temperature, H₂SiF₆ can decompose to SiF₄, and SiF₄ is easy to volatilise (boiling point: ~86 °C).

3.3.2. Results

A typical curve of dissolution kinetics of aggregates in HF is given in Fig. 2. The curve increases with the reaction time and two different phases are observed: a rapid dissolution (phase I) followed by a constant rate of dissolution characterised by a linear evolution (phase II). In phase I, the high reaction rate lasts about 2 h (between 1 and 4 h) and is mainly due to the quick dissolution of the reactive phase. In phase II, the reaction rate slows down, but the reaction still keeps an upward trend even after 24 h. This phase is usually considered to be representative of the attack of crystallised minerals such as quartz. The reactive phase is estimated by extrapolating the linear trend to $t = 0$, since it can be assumed that the crystallised phases are also dissolved from the beginning.

The kinetics of dissolution of the aggregates in HF (O, Q and QA) or in HF + HCl (SL) are given in Fig. 15. The two-phase evolution obtained for the aggregates is consistent with the works of [20,21], who worked on pozzolans. The results deduced from these curves (reactive silica content, end of phase I and dissolution rate of crystalline phase) are shown in Table 4.

As for the other methods, O gave the highest value, much higher than the other aggregates. SL and Q were in the same range, and also showed a similar reactivity in expansion tests (Fig. 11). QA gave the lowest value, in accordance with the fact that this aggregate is considered as poorly reactive.

A supplementary test with HF only was made for the siliceous limestone. A value of 5.3% was found, compared to 6.9% when HF–HCl was used. This 20% difference cannot be caused by the attack by the added HCl, because Liang and Readey [27] found that the addition of 1 mol/l HCl in HF solution did not change the dissolution of silica in fused silica and quartz. The difference may be attributed to the fact that, under the effect of HCl acid, the calcite is dissolved and then more silica was released from the enclosure of calcite (no pre-treatment was made for acid attacks) and participated in the reaction with HF. HF also dissolved calcite, but the production of CaF₂ which has low solubility, was likely to precipitate around the silica and prevent it from being attacked. Thus, it was considered that the result of HF + HCl was more reliable.

The dissolution rates of crystalline phase for the materials containing mostly silica (O, Q, and QA) were of the same order of magnitude (between 0.28 and 0.41%/h) and were controlled by the dissolution of quartz. The differences probably depended on the properties of the attacked crystallized phases, such as the surface area and the porosity, which controlled the diffusion process of the solution in the aggregate. In the case of siliceous limestone, the slower rate of dissolution (0.15%/h) was probably due to the presence of calcite, which made the silica more difficult to reach than in the other aggregates.

3.4. Comparison of the methods

The three methods presented in the previous section were effective in attacking silica in aggregates (Fig. 16) but, as discussed, some doubts remained about the nature of the dissolved silica. It is important to know if the silica quantified by these methods is only the part of the silica that is reactive, i.e. the one responsible of the degradation of concrete due to ASR, or if a part of the crystallised silica, which should remain stable in the long term in a cement-based material, is also dissolved.

The reliability of the methods is now discussed by comparing, in Fig. 17, the results of the three methods (Fig. 16) with the asymptotic expansions measured with the mortar-bar test (Fig. 11).

3.4.1. NaOH–HCl

Basic attack is thought to be representative of the real structure environment. However, this method did not seem reliable, for many reasons:

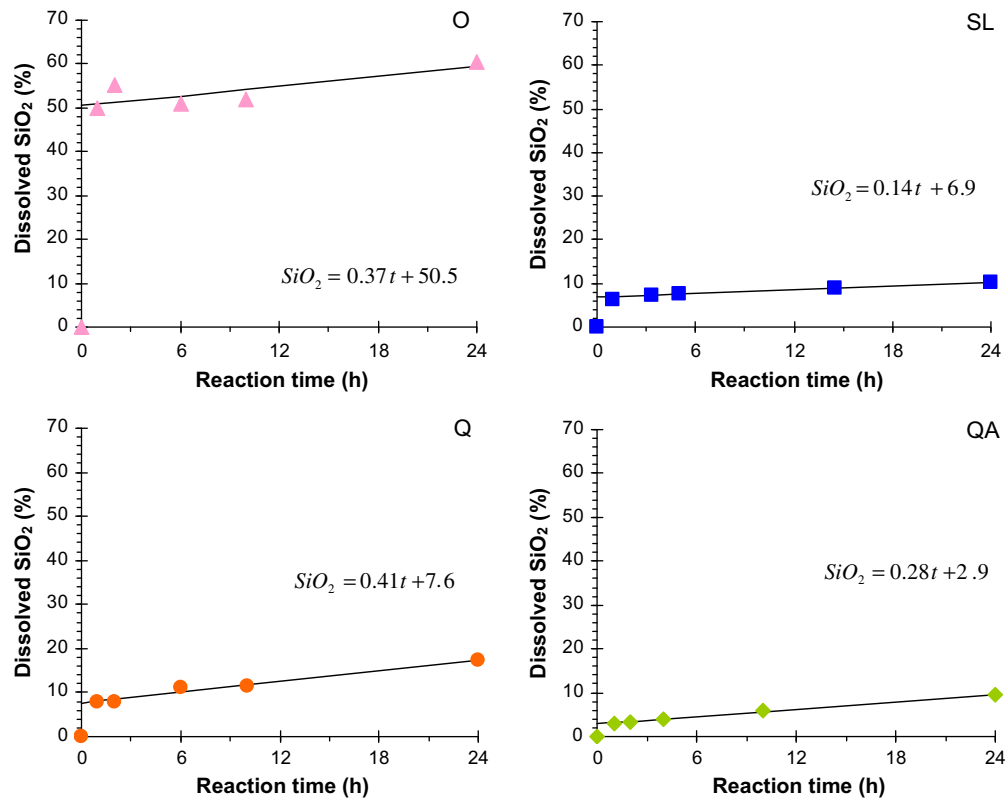


Fig. 15. Evolution of dissolved silica in HF as a function of time at 4 °C, L/S = 200 ml/g (a) opal, (b) siliceous limestone, (c) quartzite, and (d) quartz aggregate.

Table 4

Results of dissolved silica in HF/HF + HCl solution at 4 °C, L/S = 200 ml/g.

	O	SL	Q	QA
Amorphous SiO ₂ (%)	50.4	6.9 ^a	7.6	2.7
End of phase I (~h)	1	3	1	2
Dissolution rate of crystalline phase (%/h)	0.38	0.14	0.41	0.28

^a HF + HCl.

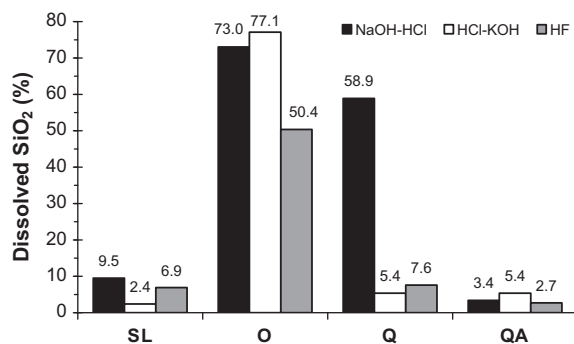


Fig. 16. Dissolved silica of each material for the three tests used.

As seen in the literature (e.g. Tucker [39]), the dissolution of silica at high pH is difficult to control and high variations of SiO₂ can be obtained for small differences of pH.

For a given aggregate, no different rates of dissolution can be distinguished (as for HF attack), which would allow the separation of the different forms of silica. Thus the dissolved silica is calculated from an asymptotic value obtained by curve fitting. Knowing that, at high temperature, the kinetics of quartz dissolution

increases rapidly [27], some concerns arose about whether this method attacked part of the well-crystallized silica. It led to an overestimation of the reactive silica available for ASR in concrete. The decrease of the temperature (from 100 to 60 °C) did not improve the results, and the duration of tests became problematic (tens of days). Since high temperatures are usually used in accelerated ASR tests, some concerns could arise about the effectiveness of evaluating reactive aggregates in mortars and concrete at these temperatures. Moreover, no correlation can be highlighted with expansion measurements (Fig. 17).

An improvement of the method would be to more accurately reproduce the pore solution of concrete that attacks the aggregates, as in the method proposed by Bulteel et al. [25]. However, this kind of method leads to the production of hydrates (which include silica), and thus makes the measurement of silica complicated and time-consuming.

3.4.2. HCl-KOH

This method is derived from the analysis of cements and standardised for fly ash (EN 450-1 [13]). It has been successively used for the measurement of the reactive part of fly ash. However, the results obtained on aggregates seem to deviate from the practical expansion results (Fig. 17). The main disadvantage seen in the present study is that the severe acid environment combined with hot conditions led to the dissolution of well-crystallised quartz (e.g. QA). With only one test at a given time, it seems impossible to distinguish between the different forms of silica. So in order to guarantee correct separation of reactive and stable silica, it seems to be preferable to use a method which gives the kinetics of dissolution.

3.4.3. HF

When compared to the former methods, the advantage of HF (or HF + HCl when calcite is the main component of the aggregate)

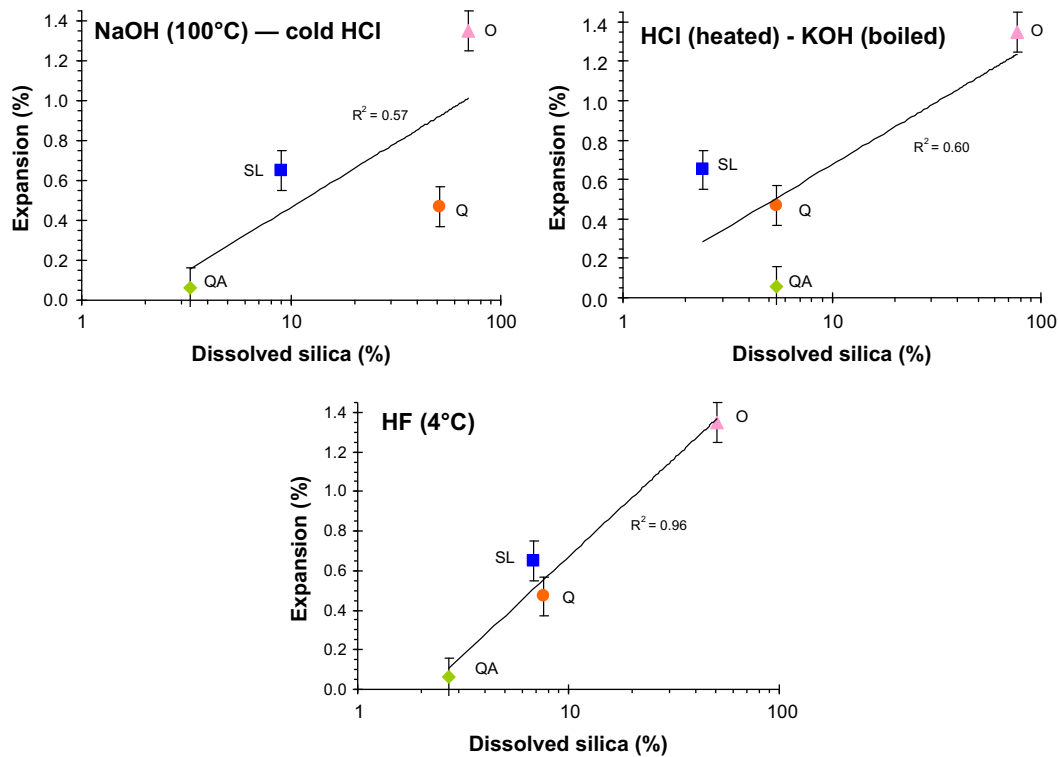


Fig. 17. Final expansion of mortar bars as a function of dissolved silica for aggregates O, Q, QA and SL, for the three methods used.

attack is that it allows the calculation of the reactive silica by dissociating the dissolution curves into two phases. These two phases are distinguished by their dissolution abilities. Thus, for the HF method, there is less problem of counting parts of quartz as reactive as mentioned in the other two methods. A good correlation is found with the expansion results, as confirmed by the value of the coefficient of determination ($R^2 = 0.96$).

Although this method is based on an acid attack, it seems to be the best compromise to quantify the active fraction of silica in alkali-silica reactive aggregates. The method is rapid (in 24 h) and simple and allows the different forms of silica to be separated.

4. Conclusion

The quantification of the reactive silica is necessary to assess the residual expansion of structures damaged by ASR. The originality of this work is to investigate three methods used to measure the reactive silica in various aggregates in the sole aim of quantifying the part of silica potentially available for ASR in concrete. The use of the real conditions of liquid/solid ratio and temperature of ASR-damaged structures would lead to long measurements; this would hardly be effective for the assessment. That is why fast methods are necessary.

Three methods were tested: one basic attack – NaOH (100 °C and 60 °C) – HCl – and two acid attacks – HCl–KOH and HF. The reactive silica was quantified in four materials, including three reactive aggregates and one non-reactive material. The results show that NaOH attack at 100 °C is more effective than attack at 60 °C but the high reaction temperature seems to cause the attack of a part of the well-crystallized minerals and thus leads to confusion between the silica which can be soluble in chemical tests and the silica which would really react with alkali in concrete (with lower liquid/solid ratio and lower temperature). HCl–KOH attack is found unsuitable since the results of reactive aggregate – Quartzite, and the non-reactive aggregate – Quartz aggregate, are the

same. Comparing the chemical quantification with the expansion results, the HF method presents the best accordance with the mortar tests. It cannot be concluded that these values of the HF method are the exact amounts of “reactive silica” because the acid attack cannot represent the real environment of alkali-silica reaction. However, this method appears to provide a reliable approach for roughly evaluating the amount of reactive silica in the material.

Finally, among the different tests, HF (or HF + HCl) attack is the best compromise since it satisfies the objectives fixed initially: a rapid (24 h) and simple test which allows the separation of reactive and non-reactive silica. Moreover, the dissolution results obtained by this method show a high correlation with expansion tests.

Acknowledgement

This work was supported by the China Scholarship Council (CSC).

References

- [1] Dent Glasser LS, Kataoka N. The chemistry of alkali-aggregate reaction. *Cem Concr Res* 1981;11(1):1–9.
- [2] Grimal E. Caractérisation des effets du gonflement provoqué par la réaction alcali-silice sur le comportement mécanique d'une structure en béton. PhD thesis. Toulouse, Université Paul Sabatier, France; 2007.
- [3] Sellier A, Bourdarot E, Multon S, Cyr M, Grimal E. Combination of structural monitoring and laboratory tests for the assessment of AAR-swelling – application to a gate structure dam. *ACI Mater J* 2009;106(3):281–90.
- [4] Duchesne J, Bérubé MA. Discussion of the paper “the effectiveness of supplementary cementing materials in suppressing expansion due to ASR – Part 1, Concrete expansion and portlandite depletion. *Cem Concr Res* 1994;24(8):1572–3.
- [5] Lagerblad B, Trägårdh J. Slowly reacting aggregates in Sweden – mechanism and conditions for reactivity in concrete, 9th ICAAR, London; 1992. p. 570–8.
- [6] Corneille A, Douillet G, Garbe JP, Leroux A, Monachon P, Moranville-Regourd M, Poitevin P, Berra M, Turriziani R, Palmer D, Graham J. Alkali-aggregate reaction in concrete dams/alcali-réaction dans les Barrages en Béton. *Bulletin of ICOLD* 79; 1991.
- [7] ASTM C289. Standard test method for potential alkali-silica reactivity of aggregates (chemical method). October; 2003.

- [8] Forest J. Recherche d'une méthode d'appréciation rapide de la réactivité des cendres volantes et des pouzzolanes additionnées au ciment. *Silicates Industriels*; 1962. p. 265–76.
- [9] Hulett LD, Weinberger AJ. Some etching studies of the microstructure and composition of large aluminosilicate particles in fly ash from coal-burning power plants. *Environ Sci Technol* 1980;14:965–70.
- [10] Richartz W. Composition and properties of fly ashes. *ZKG – Zem Kalk Gips* 1984;84(2):62.
- [11] Sivapullaiah PV, Prashanth JP, Sridharan A, Narayana BV. Reactive silica and strength of fly ashes. *Geotech Geol Eng* 1998;16:239–50.
- [12] Mehta PK. Siliceous ashes and hydraulic cements prepared therefrom. *US Patent* 4,105,459; 1978.
- [13] AFNOR, NF EN 450–1. Cendres volantes pour béton; October 2005.
- [14] Badogiannis E, Papadakis VG, Chaniotakis E, Tsivilis S. Exploitation of poor Greek kaolins: strength development of metakaolin concrete and evaluation by means of *k*-value. *Cem Concr Res* 2004;34(6):1035–41.
- [15] Cyr M, Coutand M, Clastres P. Technological and environmental behavior of sewage sludge ash (SSA) in cement-based materials. *Cem Concr Res* 2007;37(8):1278–89.
- [16] Papadakis VG, Antiohos S, Tsimas S. Supplementary cementing materials in concrete: Part II: A fundamental estimation of the efficiency factor. *Cem Concr Res* 2002;32(10):1533–8.
- [17] Payá J, Monzo J, Borrachero MV, Ordonez LM. Determination of amorphous silica in rice husk ash by a rapid analytical method. *Cem Concr Res* 2001;31(2):227–31.
- [18] Diamond S. Particle morphologies in fly ash. *Cem Concr Res* 1986;16(4):569–79.
- [19] Iler RK. The chemistry of silica. New York: John Wiley & Sons, Inc.; 1979.
- [20] Murat M, Arnaud Y. Dissolution d'une cendre silico-alumineuse dans HF dilué influence du broyage. *Silic Indus* 1988;3–4:43–8.
- [21] Pichon H, Gaudon P, Benhassaine A, Eterradosi O. Caractérisation et quantification de la fraction réactive dans les pouzzolanes volcaniques. *Bulletin Des Laboratoires des Ponts et Chaussées*; 1996. 201. p. 29–37.
- [22] Kreshkov AP, Chivikova AN, Zagorovskaya AA. A rapid method for determining free amorphous silica in clay. *J Anal Chem URSS* 1965;20:1295–6.
- [23] AFNOR XP P18–594. Granulats – Méthodes d'essai de réactivité aux alcalis (aggregates – test methods on reactivity to alkalis); February 2004.
- [24] AFNOR NF P18–454. Réactivité d'une formule de béton vis-à-vis de l'alcali-réaction; December, 2004.
- [25] Bulteel D, Garcia-Diaz E, Vernet C, Zanni H. Alkali-silica reaction: a method to quantify the reaction degree. *Cem Concr Res* 2002;32:1199–206.
- [26] Goto K. *J Chem Soc Jpn Pure Chem Sect* 1955;76:1364.
- [27] Liang DT, Readey DW. Dissolution kinetics of crystalline and amorphous silica in hydrofluoric-hydrochloric acid mixtures. *J Am Ceram Soc* 1987;70(8):570–7.
- [28] Multon S, Cyr M, Sellier A, Diederich P, Petit L. Effect of aggregate size and alkali content on ASR expansion. *Cem Concr Res* 2010;40:508–16.
- [29] Jones JB, Segnit ER. The nature of opal I nomenclature and constituent phases. *Australian J Earth Sci* 1971;18(1):57–68.
- [30] Wilson MJ, Russel JD, Tait JM. A new interpretation of the structure of disordered α -cristobalite. *Contrib Mineral Petrol* 1974;47(1):1–6.
- [31] Guédon-Dubied JS, Cadoret G, Durieux V, Martineau F, Fasseu F, Van Overkeke V. Etude du calcaire Tournaisien de la carrière Cimescaut à Antoing (Belgique). Analyse pétrographique et chimique et réactivité aux alcalins. *Bulletin des Laboratoires des Ponts et Chaussées*; 2000. 226. p. 57–66.
- [32] Sims I, Nixon P. RILEM recommended test method AAR-I: detection of potential alkali-reactivity of aggregates – Petrographic method. *Mater Struct* 2003;36:480–96.
- [33] Broekmans MATM. Structural properties of quartz and their potential role for ASR. *Mater Charact* 2004;53:129–40.
- [34] Paul A. Chemistry of glasses. Chapman and Hall; 1982.
- [35] Garcia-Diaz E, Riche J, Bulteel D, Vernet C. Mechanism of damage for the alkali-silica reaction. *Cem Concr Res* 2006;36:395–400.
- [36] Dron R, Brivot F. Thermodynamic and kinetic approach to the alkali-silica reaction. Part 2: Experiment. *Cem Concr Res* 1993;23(1):93–103.
- [37] AFNOR NF EN 196–2. Method of testing cement, part2: Chemical analysis of cement; April 2006.
- [38] Budd SM, Frackiewicz J. *Phys Chem Glass* 1962;3:116.
- [39] Tucker ME. Sedimentary petrology: an introduction to the origin of sedimentary rocks. Wiley-Blackwell; 2001. p.262.